the plant journal

SEB SOCIETY FOR EXPERIMENTAL BIOLOGY

The Plant Journal (2024) doi: 10.1111/tpj.16665

The dual role of the RETINOBLASTOMA-RELATED protein in the DNA damage response is coordinated by the interaction with LXCXE-containing proteins

Jorge Zamora Zaragoza[1,2], Katinka Klap[1], Renze Heidstra[1], Wenkun Zhou[1,3] and Ben Scheres[1,2,*]

[1]*Laboratory of Molecular Biology, Department of Plant Sciences, Wageningen University and Research, 6708 PB, Wageningen, The Netherlands,*

[2]*Department of Biotechnology, Rijk Zwaan Breeding B.V., Eerste Kruisweg 9, 4793 RS Fijnaart, The Netherlands, and*

[3]*State Key Laboratory of Plant Physiology and Biochemistry, College of Biological Sciences, China Agricultural University, Beijing 100193, China*

Received 8 February 2022; revised 10 January 2024; accepted 18 January 2024.

*For correspondence (e-mail ben.scheres@wur.nl).

SUMMARY

Living organisms possess mechanisms to safeguard genome integrity. To avoid spreading mutations, DNA lesions are detected and cell division is temporarily arrested to allow repair mechanisms. Afterward, cells either resume division or respond to unsuccessful repair by undergoing programmed cell death (PCD). How the success rate of DNA repair connects to later cell fate decisions remains incompletely known, particularly in plants. The *Arabidopsis thaliana* RETINOBLASTOMA-RELATED1 (RBR) protein and its partner E2FA, play both structural and transcriptional functions in the DNA damage response (DDR). Here we provide evidence that distinct RBR protein interactions with LXCXE motif-containing proteins guide these processes. Using the N849F substitution in the RBR B-pocket domain, which specifically disrupts binding to the LXCXE motif, we show that these interactions are dispensable in unchallenging conditions. However, N849F substitution abolishes RBR nuclear foci and promotes PCD and growth arrest upon genotoxic stress. NAC044, which promotes growth arrest and PCD, accumulates after the initial recruitment of RBR to foci and can bind non-focalized RBR through the LXCXE motif in a phosphorylation-independent manner, allowing interaction at different cell cycle phases. Disrupting NAC044-RBR interaction impairs PCD, but their genetic interaction points to opposite independent roles in the regulation of PCD. The LXCXE-binding dependency of the roles of RBR in the DDR suggests a coordinating mechanism to translate DNA repair success to cell survival. We propose that RBR and NAC044 act in two distinct DDR pathways, but interact to integrate input from both DDR pathways to decide upon an irreversible cell fate decision.

Keywords: DNA damage response (DDR), programmed cell death (PCD), RETINOBLASTOMA-RELATED PROTEIN (RBR), LXCXE motif, NAC044.

INTRODUCTION

Living organisms encounter daily challenges to genome integrity that jeopardize their survival and reproduction. In response to intrinsic or environmental threats (Chen et al., 2019; Tsegay et al., 2019; Yi et al., 2014), eukaryotic DNA damage triggers a variety of responses collectively known as DNA damage response (DDR). Extensive investigation of the DDR pathways has shown highly conserved outcomes after DNA damage in eukaryotes (Clay & Fox, 2021; Nisa et al., 2019). The ATM/ATR kinases initiate a phosphorelay system to tag the damaged site, pause the cell cycle, and repair the lesion. If the damage persists, cells activate a suicidal program to avoid propagating mutations (Chen, 2016; Ciccia & Elledge, 2010; Hu et al., 2016; Kim et al., 2019; Lanz et al., 2019; Waterworth et al., 2019). In animals, the DDR is largely mediated by p53, a transcription factor that activates the cell cycle arrest and DNA repair programs, and if necessary, senescence and apoptosis (Chen, 2016; Kastenhuber & Lowe, 2017; Williams & Schumacher, 2016). In plants, no p53 orthologs have been found, and DDR relies on the functional analog SUPPRESSOR OF GAMMA RESPONSE1 (SOG1), a member of the plant-specific NAC-transcription factor family (NAM-ATAF-CUC; Bourbousse et al., 2018; Mahapatra & Roy, 2020; Yoshiyama et al., 2009).

Previous studies identified direct and indirect targets of SOG1 upon DNA damage in *Arabidopsis thaliana*

(Bourbousse et al., 2018; Ogita et al., 2018). Besides activating the majority of the DNA repair genes, SOG1 represses cell cycle and induces cell death by directly activating *NAC044* and *NAC085*, the closest *SOG1* paralogs (Bourbousse et al., 2018; Ogita et al., 2018; Takahashi et al., 2019). NAC044/NAC085 stabilize MYB3R3 repressor proteins that in turn bind to the M phase-specific activator sequence (MSA) present in G2/M gene promoters, arresting cell division (Chen et al., 2017; Kobayashi et al., 2015; Takahashi et al., 2019). However, how NAC044/NAC085 induces cell death after DNA injury is less clear.

In recent years, the RETINOBLASTOMA-RELATED1 protein (RBR), a homolog of the human tumor suppressor pRb, emerged as a central player in the DDR acting in parallel to SOG1 (Biedermann et al., 2017; Bouyer et al., 2018; Cruz-Ramírez et al., 2012; Horvath et al., 2017). RBR is a multifunctional protein that integrates environmental information into cell cycle and developmental programs by interacting with a plethora of transcriptional and chromatin regulators (Cruz-Ramírez et al., 2012; Desvoyes, De Mendoza, et al., 2014; Gutzat et al., 2012; Harashima & Sugimoto, 2016; Johnston et al., 2008; Perilli et al., 2013). In proliferating cells, RBR binds to E2F-DP heterodimeric transcription factors to prevent S-phase onset until CYCLIN D-CDKA kinases phosphorylate RBR to release E2F-DP, allowing cell cycle progression (Berckmans & De Veylder, 2009; De Veylder et al., 2002; Desvoyes, Fernández-marcos, et al., 2014; Magyar et al., 2012; Polit et al., 2012).

Reduction of RBR levels leads to genome instability, hypersensitivity to DNA-damaging treatments, and cell death (Biedermann et al., 2017; Cruz-Ramírez et al., 2013; Horvath et al., 2017). Upon DNA damage, RBR together with E2FA regulates the expression of repair genes and mediates the localization of the RAD51 repair protein to DNA damage sites, visualized as nuclear foci where other proteins such as histone γH2AX, E2FA, and BRCA1 co-localize with RBR (Biedermann et al., 2017; Bouyer et al., 2018; Horvath et al., 2017). Thus, it is likely that RBR plays both a structural role in DDR and a transcriptional role in mediating DNA damage-induced PCD. The SOG1 and RBR DDR pathways act in parallel, but how they cross-talk is less clear.

RBR belongs to the 'pocket protein' family, characterized by the A- and B-pocket subdomains that fold into the central 'pocket domain', an N-domain, a C-terminal region, and multiple sites for CDK-mediated phosphorylation (Desvoyes & Gutierrez, 2020; Dick & Rubin, 2013; Gutzat et al., 2012; Rubin, 2013). Pocket-protein functions rely on their ability to form protein interactions regulated by phosphorylation (Dick & Rubin, 2013; Narasimha et al., 2014; Sanidas et al., 2019). E2Fs bind to the A-B subdomains interface, while CYCLIN D proteins, chromatin modifiers, and several transcription factors bearing the conserved LXCXE motif dock in the LXCXE-binding cleft located at the B-subdomain (DeCaprio, 2009; Flemington et al., 1993; Helin et al., 1993). A point mutation that specifically disrupts pRB-LXCXE interactions fails to irreversibly arrest cell division in human cell lines (Chen & Wang, 2000), and hampers the anti-tumorigenic activity of pRB after induced DNA damage in mice (Bourgo et al., 2011). Here, we used the same amino acid change, N849F, to dig deeper into the molecular determinants underlying distinct *Arabidopsis thaliana* RBR roles during DDR. We show that the ability of RBR to interact with LXCXE-containing proteins is crucial to withstand DNA damage. We provide evidence that an LXCXE-containing protein recruits RBR to nuclear foci early after DNA damage induction. RBR also interacts with NAC044 in a LXCXE-dependent and phosphorylation-independent manner. Specific disruption of RBR-NAC044 interaction revealed that the SOG1 and RBR pathways converge on the regulation of cell death. Collectively, our results support the existence of an LXCXE-mediated mechanism to coordinate the dual role of RBR during the DDR and its cross-talk with the SOG1 pathway.

RESULTS

RBR interacts with LXCXE proteins to function in the DNA damage response

The ability of mammalian pRB to interact with LXCXE proteins is dispensable under ideal growth conditions, but it is essential when DNA is damaged (Bourgo et al., 2011). To investigate the role of RBR-LXCXE interactions in the plant DDR, we analyzed the effect of mutating asparagine (N) 849 to phenylalanine (F) in Arabidopsis RBR, hereafter referred to as RBR^{NF} (Cruz-Ramírez et al., 2013). N849 is a conserved residue of the RBR LXCXE-binding cleft located in the B-pocket subdomain (Gutzat et al., 2012), and other studies in mammals (Bourgo et al., 2011; Chen & Wang, 2000) and Arabidopsis (Cruz-Ramírez et al., 2013) have used the NF allele to disrupt LXCXE interactions. Since *rbr* null mutations are lethal (Ebel et al., 2004), we transformed a transgenic *pRBR::*RBR^{NF}*:vYFP* (**RBR^{NF}*-YFP*) construct into our previously reported 35S::amiGO-RBR line (hereafter amiGO), a ubiquitously expressed RBR-targeted artificial micro RNA that strongly reduces endogenous RBR activity but permits complementation with transgenic *RBR* variants lacking the 3′UTR (Cruz-Ramírez et al., 2013).

Although RBR^{NF}-YFP displayed a brighter signal than RBR-YFP, the roots of both variants grew similarly normal in standard conditions (Figure 1a). However, only RBR-YFP was able to sustain growth on medium supplemented with zeocin (Figure 1b), a radio-mimetic genotoxic agent that creates double-strand breaks (DSB) in the DNA (Kim et al., 2019). A recovery period after zeocin pulse treatment revealed that roots carrying the *RBR*^{NF}*-YFP* allele were unable to cope with DNA damage, similarly sensitive as

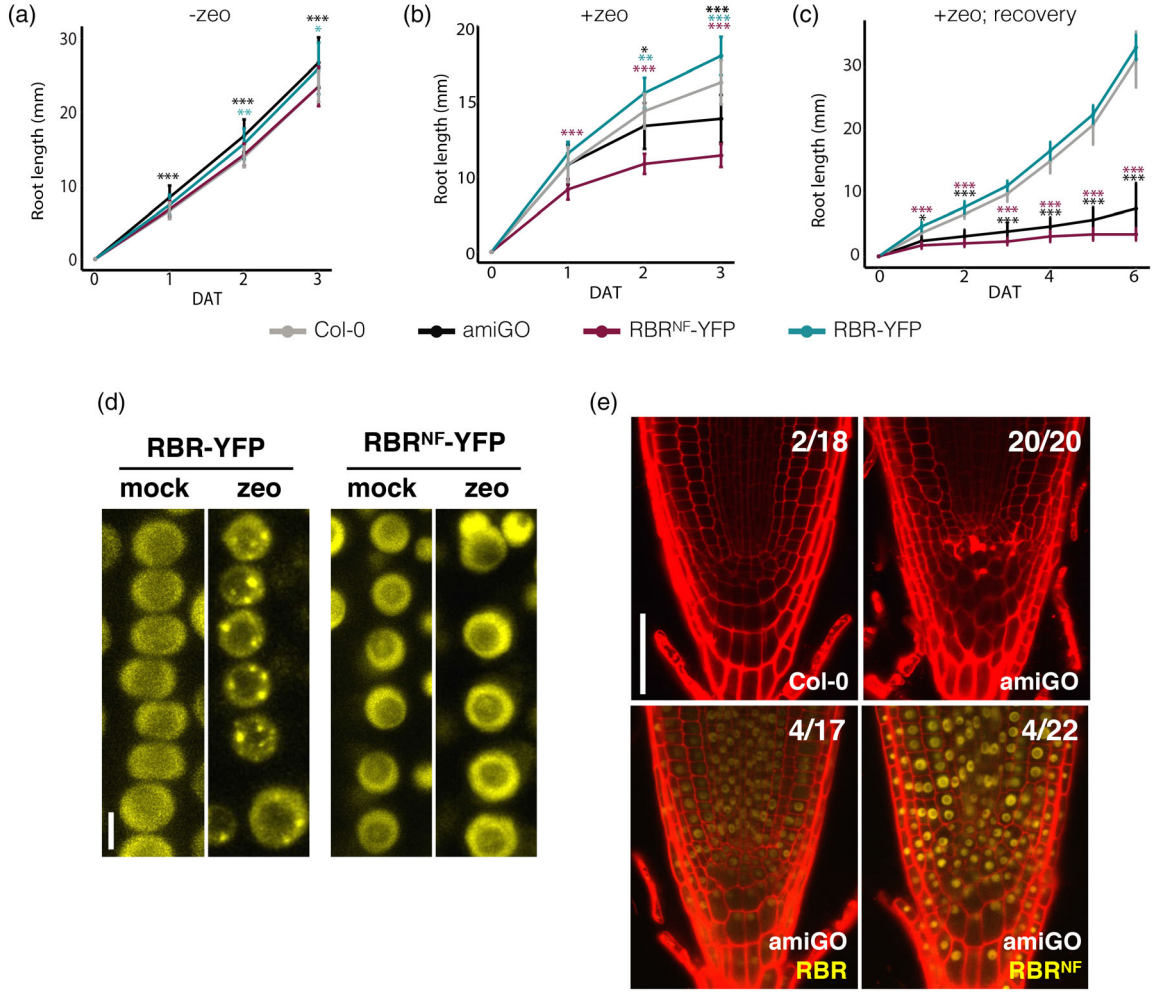

Figure 1. The LXCXE motif interacting domain of RBR is needed to cope with DNA damage.
(a–c) Root growth comparison of Col-0, amiGO, RBR-YFP, and RBR^{NF}-YFP measured in millimeters (mm). Seedlings germinated and grown on 0.5 GM medium for 4–5 days were transferred to 0.5 GM medium without (a) or with (b) 3 μg ml^{-1} zeocin (zeo) for 3 days after transfer (dat), or incubated on 10 μg ml^{-1} zeo for 20 h and transferred again to 0.5 GM for recovery over 6 dat (c). Data in (a, b) presented as mean ± SD of two independent replicates, in (c) a single representative replicate is presented due to high variability in zeocin treatments. $10 < n < 17$. ***$P < 0.001$, **$P < 0.01$, *$P < 0.05$.
(d) Representative maximum-intensity projections of z-stack images from RBR-YFP and RBR^{NF}-YFP living roots nuclei (genetic background: amiGO) after 16 h incubation in 0.5 GM medium supplemented with without (mock) or with 10 μg ml^{-1} zeo.
(e) Cell death visualized by confocal imaging of longitudinal sections of propidium iodide (PI)-stained root tips 8 days post germination (dpg) on 0.5 GM medium without zeo (PI selectively permeates dead cells, forming characteristic red spots); numbers indicate roots presenting dead cells in Col-0, amiGO, RBR-YFP and RBR^{NF}-YFP.
RBR-YFP and RBR^{NF}-YFP are in the amiGO genetic background in a–d. Scale bars, 5 μM in (d), 50 μM in (e).

the amiGO if not more (Figure 1c). In both cases, the meristem of the *amiGO* and *RBR^{NF}-YFP* roots collapsed (Figure S1a,b), suggesting that the ability to interact with LXCXE-containing proteins is essential for Arabidopsis RBR to confer protection against induced DNA damage.

Since RBR aggregates in nuclear foci with histone γH2AX, E2FA, and repair proteins RAD51 and BRCA1 upon induced DSB (Biedermann et al., 2017; Horvath et al., 2017), we asked whether the inability of RBR^{NF}-YFP roots to recover from DNA damage relates to this process. Strikingly, zeocin-induced foci formation was completely abolished in RBR^{NF}-YFP (Figure 1d; Figure S1c,d), suggesting that an LXCXE-containing protein is required to tether RBR to DSB. A conserved LXCXE motif in RAD54 (Figure S2a), a DNA repair protein that also forms repair foci with RAD51 in Arabidopsis (Hirakawa et al., 2017; Hirakawa & Matsunaga, 2019), led us to test whether RAD54 recruits RBR to foci. We failed to demonstrate that RBR and RAD54 bind directly (Figure S2b), and no co-localization of RAD54 and RBR in zeocin-induced foci was observed, in contrast to the highly co-localized RBR/E2FA foci (Figure S2c–h). Since RBR forms foci in the absence of RAD54 (Figure S2i), RAD54 is unlikely to recruit RBR to the DNA damage sites. In sum, the LXCXE-binding cleft is

crucial for RBR foci formation and tethering by an as yet unidentified LXCXE-containing protein.

Root tips with reduced RBR levels display cell death even in unchallenging conditions, likely due to intrinsic genome instability (Biedermann et al., 2017; Cruz-Ramírez et al., 2013; Horvath et al., 2017; Wildwater et al., 2005), but whether this phenotype relates to defective foci dynamics is unknown. Since RBR^{NF}-YFP rescued this phenotype observed in amiGO roots to the same extent as RBR-YFP (Figure 1e), we conclude that the ability of RBR to form nuclear foci is dispensable to promote cell survival in standard growth conditions.

Phosporylation state independent interaction of RBR with NAC044 through a conserved LXCXE motif

In a Y2H screening of the Arabidopsis transcription factors library (Pruneda-Paz et al., 2014) we identified NAC044 as a strong RBR interactor (preprint: Zamora-Zaragoza et al., 2021). *NAC044* and *NAC085* are the closest homologs and direct transcriptional targets of SOG1, (Ogita et al., 2018; Takahashi et al., 2019). We noticed that NAC044 contains an LXCXE motif in the C-terminus that is conserved among NAC044 orthologs in monocots and dicots species but is absent in NAC085 and divergent in SOG1 orthologs (Figure 2a,b). Noteworthy, the LXCXE motif in NAC044 is identical to that of RAD54 (Figure 2a; Figure S2a). To test the RBR binding capacity of the NAC044 LXCXE motif, we performed Y2H assays. Figure 2 (c) shows that E2FC binds to RBR and RBR^{NF}, but NAC044 failed to interact with RBR^{NF}, and SOG1 was unable to interact with RBR. When the LXCXE motif in NAC044 was changed into GXCXG (hereafter $NAC044^{GCG}$) the interaction with RBR was abolished (Figure 2c), confirming a similar experiment published previously (Lang et al., 2021). Split-luciferase assays showed that, while E2FA, E2FB, and E2FC interacted *in planta* with both RBR and RBR^{NF} (Figure S3a), NAC044-RBR binding was disrupted by either RBR^{NF} or $NAC044^{GCG}$ mutations (Figure 2d). Moreover, RBR and NAC044 interacted in an LXCXE-dependent manner upon zeocin treatment as shown by a split-luciferase assay in stable transgenic Arabidopsis seedlings (Figure S3b).

RBR protein interactions are generally regulated by phosphorylation on multiple sites. While both E2FC and NAC044 interacted with a fully phospho-defective RBR variant, a phospho-mimetic version of RBR (where replacement of all phospho-sites by aspartic or glutamic acid resembles constitutive phosphorylation) disrupted the binding to E2FC but surprisingly not to NAC044 (Figure 2e). Since NAC044 fosters G2/M cell cycle arrest (Takahashi et al., 2019), and RBR is phosphorylated at the G1/S-phase transition (Boniotti & Gutierrez, 2001; Nakagami et al., 2002), there is a functional explanation for the ability of NAC044 to bind the hyper-phosphorylated form of RBR. Altogether, our results demonstrate that RBR interacts with NAC044 in an LXCXE-dependent manner but independent of the RBR phosphorylation state –which is relevant in the likely scenario where both proteins act together after the G1/S phase transition.

RBR foci formation and clearing after DNA damage occurs prior to peak accumulation of NAC044

To study the function of *NAC044 in situ*, we generated *NAC044* transcriptional and translational reporters driven by a promoter comprising the intergenic region and harboring the SOG1 binding site, an MSA element, and an E2F-binding box (Figure S4a). The expression of transgenic *pNAC044::GUS* and *pNAC044::3GFP-NLS* reporters resembled the previously reported expression pattern in the root tip (Takahashi et al., 2019), characteristic of DNA damage-induced and cell cycle-regulated genes (Figure S4b) and contrasting with its age-dependent expression in the floral organ abscission zone (Figure S4c).

The protein product of the *pNAC044::NAC044:GFP* transgene (hereafter *NAC044-GFP*) never formed foci after a zeocin treatment that promoted RBR focus formation and NAC044-GFP accumulation in the same nuclei (Figure S4d), indicating that NAC044 is unable to bind focalized RBR. Moreover, RBR formed foci in the absence of NAC044 (Figure S4e). Therefore, NAC044 is not the recruiter of RBR at foci, and more likely acts with RBR in the later transcriptional response rather than in the structural aspect of DNA repair. Thus, these RBR roles are separated in the subnuclear space by LXCXE-binding constraints.

Figure 2. RBR interacts with NAC044 through a conserved LXCXE motif regardless of RBR phosphorylation state.
(a) Protein sequence alignment of Arabidopsis NAC044 (ANAC044) and SOG1 orthologs in the indicated plant species showing the fragment with LXCXE and LXXCXE/D motifs highlighted. No ANAC085 orthologs lacking an LXCXE motif were found in these species.
(b) Schematic representation of NAC044 protein organization showing the relative positions of the NAM domain and LXCXE motif.
(c) Yeast two-hybrid analysis showing that BD-RBR, but not BD-RBR^{NF}, interacts with AD-NAC044, and neither of them binds AD-SOG1 nor an LXCXE-to-GXCXG-mutated AD-NAC044 protein ($NAC044^{GCG}$). AD-E2FC and empty vector (AD) are positive and negative controls, respectively. Transformant yeast was dropped onto SD/-L/-W (-LW), SD/-L/-W/-H/+1.5mM3AT (-LWH). AD and BD, GAL4 activation domain, and DNA binding domain, respectively.
(d) Split Luciferase assay of RBR binding to NAC044 *in planta*. *N. benthamiana* leaves were co-infiltrated with the plasmid combinations and in the order indicated by dashed-line divided quadrants. Luciferase activity and a bright field images are shown. Representative images of six independent replicates.
(e) Yeast two-hybrid analysis reveals that NAC044 interacts with a non-phosphorylatable RBR mutant (phospho-defective RBR) and phospho-mimmetic RBR. All 16 putative CDK-phospho-sites in RBR were mutated to Ala (phospho-defective) or to either Asp or Glu (Phospho-mimmetic). Transformant yeast were dropped onto SD/-L/-W (−LW), SD/-L/-W/-H/+1.5mM3AT (−LWH), SD/-L/-W/-H/-A (−LWHA). Data shown are representative of three independent replicates and belongs to a larger Y2H screening reported in (preprint: Zamora-Zaragoza et al., 2021).

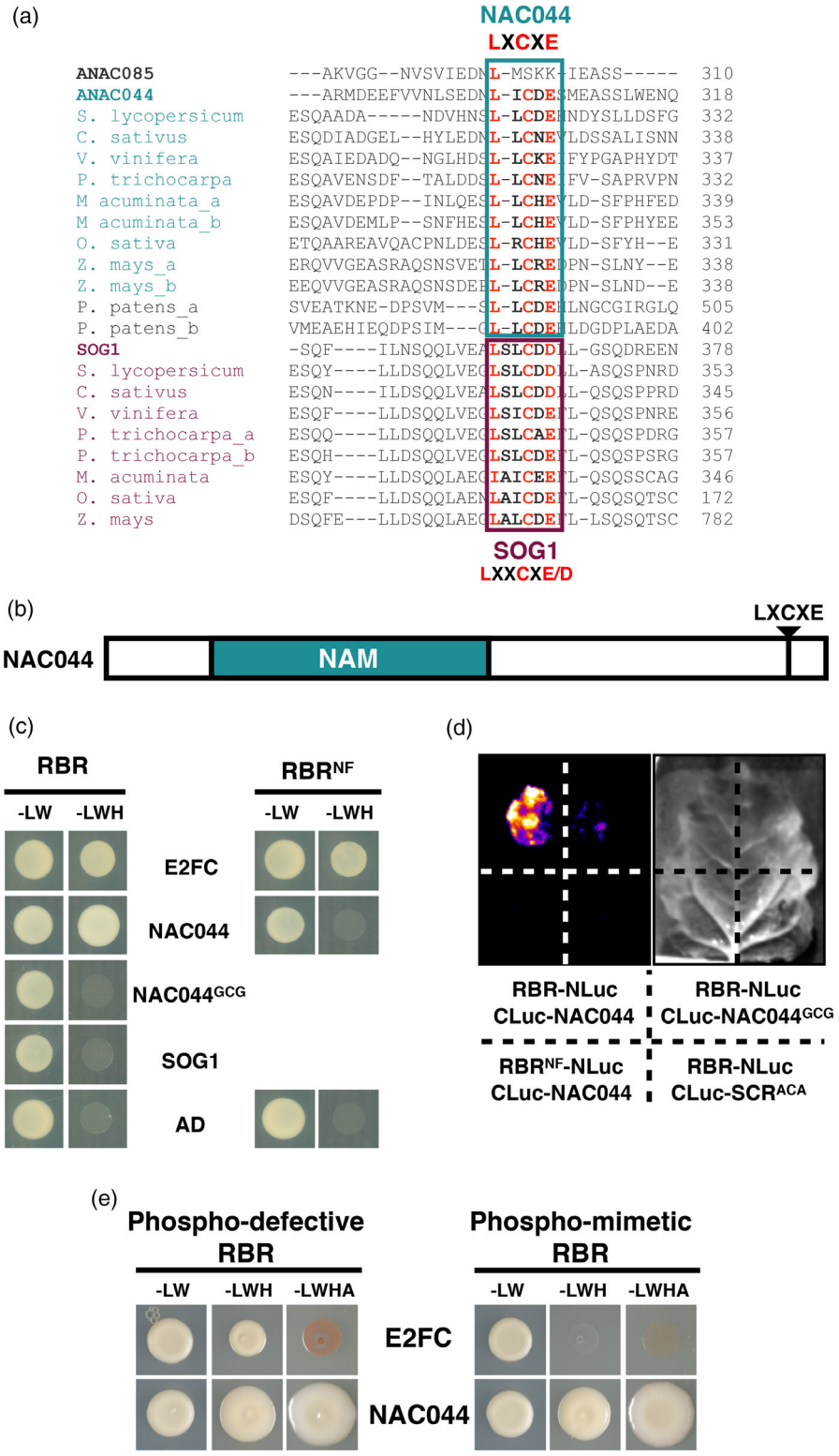

RBR functions might also have a temporal separation. RBR foci formed immediately after a short exposure to zeocin and rapidly increased within 1 h (Figure 3a,b), whereas a long treatment induced a large amount of RBR foci that cleared out by more than half in 4 h, and almost completely within 8 h of recovery (Figure 3c,d).

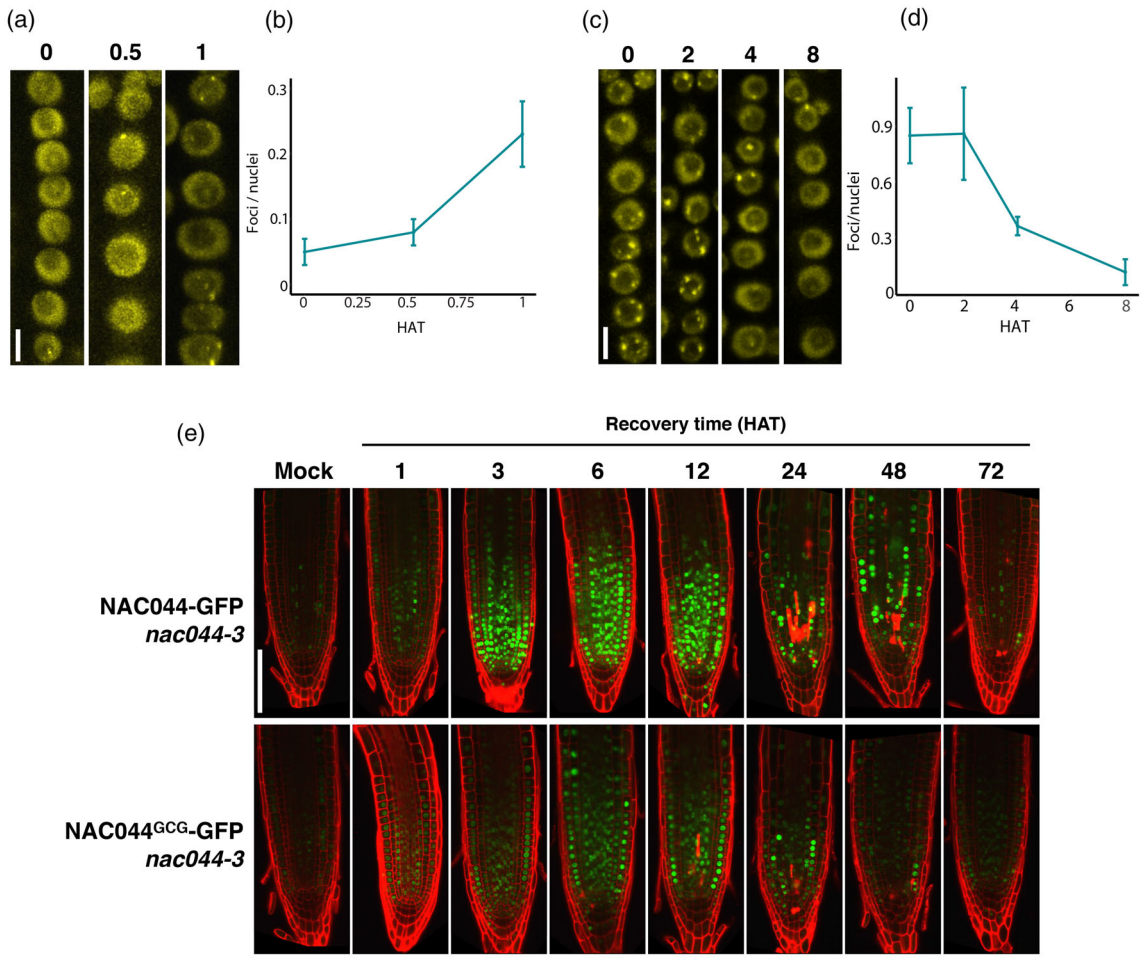

Figure 3. RBR foci are processed faster than NAC044 expression induction by DNA damage.
(a–d) RBR-YFP foci at 0, 0.5, and 1 h (a, b) or 0, 2, 4, 8 (c, d) hours after zeo treatments (HAT): 20 μg ml^{-1} zeo for 2 h (a, b) and 10 μg ml^{-1} zeo for 16 h (c, d) are timepoint 0. Seedlings were transferred to 0.5 GM for the indicated recovery time (HAT) before imaging. Representative maximum-intensity projections of z-stack images from RBR-vYFP living roots nuclei (a, c) and quantification of nuclear foci divided by the number of nuclei (b, d). Data in (b, d) presented as mean ± SD. In (b) $n > 3$ roots, total nuclei per time point >1000; in (d) $n > 4$, total nuclei per time point >2000.
(e) Representative confocal images of longitudinal sections of roots from *nac044-3* complementing translational fusions pNAC044::gNAC044:GFP and pNAC044::gNAC044^{GCG}:GFP after 2 h incubation on 20 μg ml^{-1} zeo. Seedlings were transferred to 0.5 GM for the indicated recovery time before imaging.
Scale bars, 5 μm in (a, c), 100 μm in (e).

Conversely, the pNAC044 transcriptional reporters increased their expression 3 h after a short zeocin treatment, peaking after 12 h, and lasting for more than 2 days (Figure S4b). The rapid RBR accumulation and clearance in foci, and the late and longer pNAC044-GUS and pNAC044:3GFP-NLS expression peaks suggest that the structural role of RBR in DNA repair occurs in an earlier phase of the DDR than its interaction with NAC044.

RBR and NAC044 act both independently in the DDR, and together to induce cell death after DNA damage

To further explore the biological relevance of the NAC044-RBR interaction, we transformed NAC044-GFP and its LXCXE-mutated version (*pNAC044::NAC044^{GCG}:GFP*; hereafter *NAC044^{GCG}-GFP*) in the genetic background of two *nac044* knock-out alleles, *nac044-3* (Figure S4f) and the reported *nac044-1* (Takahashi et al., 2019), both exhibiting a similar insensitivity phenotype to DNA damage (Figure S4g–i). Both *NAC044-GFP* and *NAC044^{GCG}-GFP* fully complemented the lack of growth inhibition in *nac044-3* when seedlings grew on sustained zeocin conditions (Figure S4i), demonstrating the functionality of the GFP-tagged transgenes, and suggesting that the NAC044 interaction with RBR is not required for root growth arrest. After a short zeocin exposure, all reporters were induced, but the translational fusions displayed a broader and earlier expression than the promoter reporters (Figure 3e; Figure S4b)—possibly due to differences in protein stability. Both NAC044-GFP and NAC044^{GCG}-GFP gradually accumulated, reaching maximum levels between 6 and 12 h,

then they gradually decreased over the course of 2 days. In accordance with its reported function, along with the GFP signal accumulation, cell death increased during the first 24 h after DNA damage induction (Figure 3e). Thus, the effect of NAC044 accumulation in the root meristem is observable well beyond the time it takes RBR to clear from foci.

We further tested the effect of a prolonged pulse of zeocin on root growth to address the physiological role of the RBR-NAC044 interaction. Whereas, extra copies of *RBR* (endogenous *RBR* and transgenic *RBR-YFP*) seemed to have a positive dosage effect on root growth (Figure S5a), RBR^{NF}-YFP imposed a strong defect in coping with DNA damage, regardless of the genetic background tested—amiGO, Col-0, and nac044-3 (Figure 1c; Figure S5a), which indicates that the insensitivity effect of the *nac044-3* mutant allele, and the protective activity of endogenous RBR on root growth after DNA damage are both overruled by RBR^{NF}-YFP. Since RBR^{NF}-YFP does not interfere with Wt RBR foci formation (Figure S1d), we conclude that RBR^{NF}-YFP displays dominant negative features upon DNA damage induction that cannot be solely explained by its inability to form foci or to interact with NAC044. Since RBR^{NF} interacts with E2FA (Figure S3a), an essential component for RBR's structural and transcriptional roles in the DDR (Horvath et al., 2017), RBR-E2FA protective activity seems to strictly require binding of another LXCXE-containing protein. As previously determined (Takahashi et al., 2019), *nac044-1* plants kept growing after zeocin treatment (Figure S5b), whereas several independent *NAC044-GFP* and *NAC044^{GCG}-GFP* transgenic lines with varying but comparable accumulation levels (Figure S5c) consistently showed over-complementation of *nac044-1* mutants (Figure S5b), suggesting that the root growth arresting function of NAC044 is restored and enhanced by both GFP-fusion proteins. Moreover, NAC044^{GCG}-GFP behaved similar to NAC044-GFP, indicating that, unlike previously proposed (Lang et al., 2021), the NAC044-RBR complex functions in a different process of the DDR than root growth arrest.

NAC044 has a second function, as it also mediates *SOG1*-dependent cell death upon DNA damage (Takahashi et al., 2019). In turn, RBR promotes cell survival in an E2FA-dependent- and *SOG1*-independent manner (Horvath et al., 2017). So we asked if, despite their opposite DNA damage induced-PCD phenotypes (Biedermann et al., 2017; Horvath et al., 2017; Takahashi et al., 2019) the SOG1 and RBR parallel pathways cross-talk via NAC044-RBR protein interaction to control PCD. As expected, *nac044-1* barely displayed cell death at 20 h of zeocin exposure (Figure 4a,b). The transgenic NAC044-GFP completely restored the induction of cell death in *nac044-1* and even over-complemented it in two transgenic lines, similar to our observation in root growth arrest. All three *NAC044^{GCG}-GFP* transgenic lines consistently showed less cell death area than any of the *NAC044-GFP* lines; two of them had slightly more cell death than *nac044-1* whereas one behaves like the null mutant; and two out of the three *NAC044^{GCG}-GFP* transgenic lines displayed significantly less cell death area than the Col-0 control (Figure 4a,b). To verify the effect of the GCG substitution on NAC044, an independent experiment that induced a more extensive damage in all genotypes clearly showed that all three *NAC044^{GCG}-GFP* transgenic lines consistently display less cell death area than Col-0 and one of them behaves similar to the *nac044-1* control (Figure S5d,e). A fourth independent transgenic line for each construct in the *nac044-3* background supports these results, with *NAC044^{GCG}-GFP* having a smaller cell death area than Col-0 and *NAC044-GFP* behaving as Wt (Figure S5f). Our results suggest that the induction of cell death upon DNA damage by NAC044 depends in part on its protein interaction with RBR.

Surprisingly, *RBR^{NF}-YFP* behaved opposite to the *NAC044^{GCG}-GFP lines*, regardless of the presence or absence of the amiGO construct (Figure 4c,d; Figure S5g,h), confirming that LXCXE-mediated functions of RBR in the DNA damage-induced PCD are complex and extend beyond its interaction with NAC044. Whether RBR binds to NAC044 or other LXCXE proteins, and the competition between such binding events, may determine its effect on PCD. Noteworthy, the introgression of *nac044-3* (Figure 4c,d) or *nac044-1* (Figure S5d,e) in the amiGO line rendered an intermediate phenotype where the cell death area was much smaller than in the amiGO, but significantly larger than in *nac044-3* or *nac044-1*, respectively. Despite the strong dominant negative effect of *RBR^{NF}-YFP* (Figure S5g,h), *nac044-3* introgression also mitigated the cell death area in the double transgenic amiGO/*RBR^{NF}-YFP* line (Figure 4c,d). Our results indicate that besides their PCD-activating function as a protein complex, *RBR* and *NAC044* also have independent and opposite roles in DNA damage-induced cell death.

DISCUSSION

Despite their independence, recent studies pointed to a complex and yet poorly understood convergence of the RBR and SOG1 DDR pathways (Bourbousse et al., 2018; Chen et al., 2017; Lang et al., 2021; Nisa et al., 2023). Here we report that the integrity of the LXCXE-binding cleft is essential for RBR to confer protection against genotoxic stress, and we provide a mechanistic insight into the cross-talk between the SOG1 and RBR pathways through the functional characterization of the RBR-NAC044 interaction. In the following paragraphs, we discuss our results in relation to the literature and propose an integrated interpretation of our findings.

Upon DNA damage, the repair machinery aggregates in highly dynamic nuclear foci (Biedermann et al., 2017; Gentric et al., 2020; Nakamura et al., 2010; Polo &

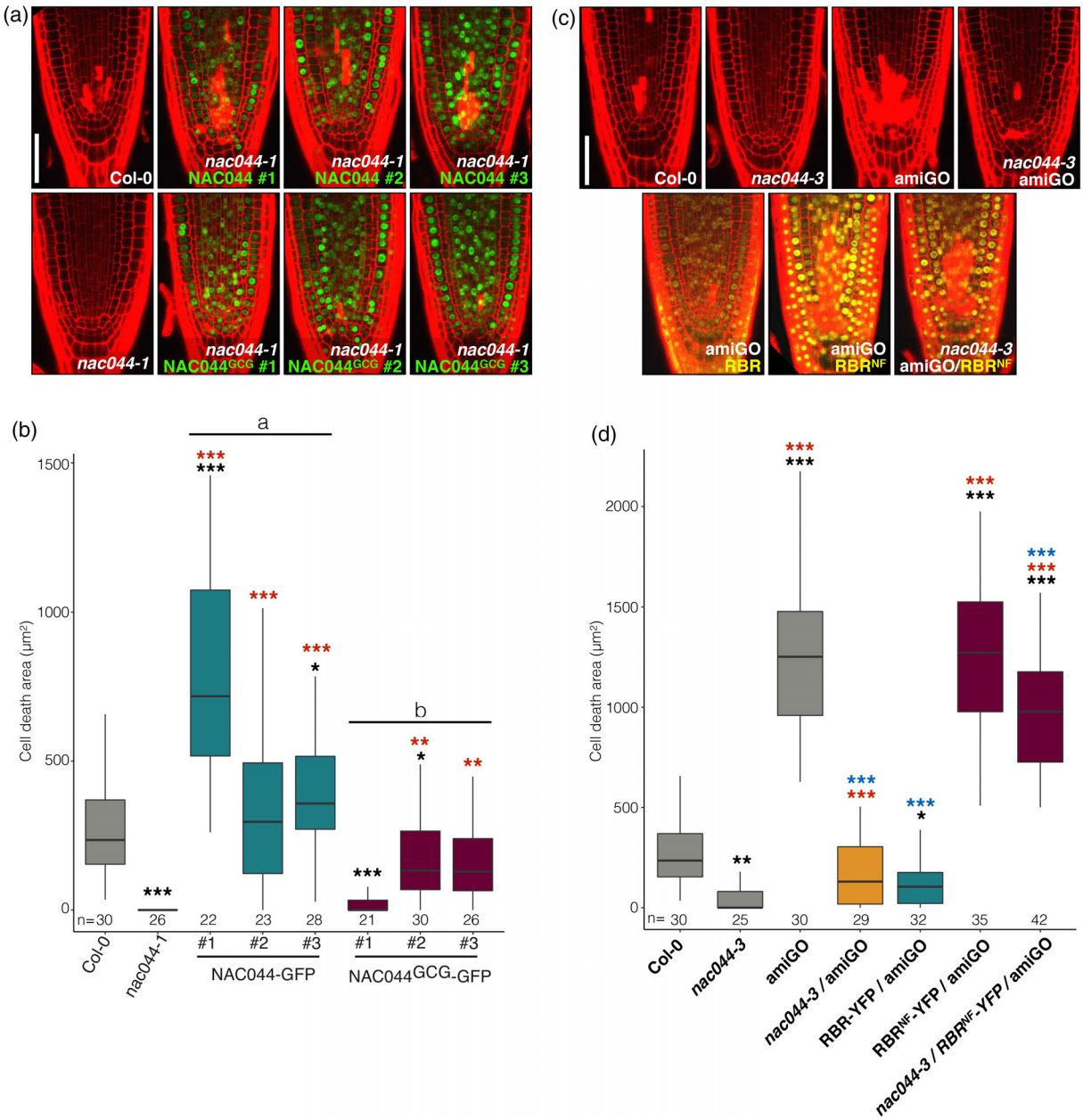

Figure 4. NAC044 interacts with RBR to induce cell death after DNA damage.

(a, c) Cell death visualized by PI accumulation (red spots formed by PI permeated in dead cells) in a representative confocal image of root tips longitudinal sections from the indicated genotypes; 5 dpg seedlings were incubated on 10 µg ml^{-1} zeo for 20 h before imaging. (a) Three independent transformant lines of NAC044-GFP and NAC044^{GCG}-GFP in *nac044-1* mutant background are shown along with the Col-0 and *nac044-1* controls. (c) Transgenic RBR-YFP and RBR^{NF}-YFP complementing the amiGO background, and the amigo × nac044-3 cross are shown along with their controls plus the triple RBR^{NF}-YFP/amiGO/*nac044-3*. Scale bar, 50 µm.

(b, d) Box plots of quantified cell death area (µm^2) in the root tips mentioned in (a) and (c). Data presented as median and interquartile range from two biological replicates, n denotes total number of scored roots. A third biological replicate showed similar results. Wilcoxon test, asterisks denote *$P < 0.05$, **$P < 0.01$, ***$P < 0.001$ as compared to controls. Controls for (b) are Col-0 (black asterisks) and *nac044-1* (red asterisks); controls D are Col-0 (black asterisks), *nac044-3* (red asterisks), and amiGO (blue asterisks). Lowercase letters in (b) indicate that all lines belonging to 'group a' are statistically different from all lines in 'group b'. Data of Col-0 control is the same for both experiments, which were performed simultaneously.

Note in (b) that two NAC044-GFP lines show increased cell death area and two NAC044^{GCG}-GFP show decreased cell death area as compared to Col-0; Figure S5 (d,e) shows an independent experiment where a more extensive damage revealed that all three NAC044-GFP lines behave similar to Col-0, whereas all three NAC044^{GCG}-GFP have reduced cell death. A fourth independent transformant of NAC044-GFP and NAC044^{GCG}-GFP in the *nac044-3* background reproduces these results (Figure S5f).

Jackson, 2011), where RBR accumulates and co-localizes with other proteins like histone γH2AX, E2FA, F-BOX-LIKE PROTEIN 17 (FBL17) and the repair proteins BRCA1 and RAD51 (Biedermann et al., 2017; Gentric et al., 2020; Horvath et al., 2017). In animals, pRb is also recruited to nuclear foci with similar kinetics as histone γH2AX, and in an E2F1-dependent manner (Vélez-Cruz et al., 2016). However, we found that RBR^{NF}-YFP was unable to accumulate in nuclear foci despite its ability to interact with E2F proteins, suggesting that in plants, an interaction between the B-pocket subdomain and, most likely, an LXCXE-containing protein recruits RBR to the DNA damage site. Interestingly, the *rbr1-2* allele, which lacks the B-pocket sub-domain, displays reduced sister chromatide cross-over and DSB-dependent foci formation of meiotic proteins during prophase I (Chen et al., 2011), highlighting the importance of the B-pocket-mediated interactions in programmed and stress-induced chromatin repair. Since *RBR^{NF}-YFP* completely restored the compromised cell survival of the amiGO line in unchallenging conditions, we conclude that, like the mammalian pRb (Bourgo et al., 2011), the ability to interact with LXCXE proteins becomes essential under specific conditions such as genotoxic stress, in part because the early structural role of RBR in DNA repair depends on such interactions.

RBR-YFP foci accumulate quickly after DNA damage and nearly 90% of these are cleared during the first 8 h of recovery, coinciding with the accumulation of NAC044-GFP, which does not form foci. Our data indicate that the main biochemical constraint for NAC044 to bind RBR is the availability of the B-pocket sub-domain, while the phosphorylation state of RBR seems irrelevant for binding, allowing these proteins to interact and exert their function throughout the cell cycle interphase. Whether focus-released RBR immediately binds NAC044, or whether a portion of RBR not recruited to foci can interact with NAC044 remains unknown, but disrupting the LXCXE motif in NAC044 leads to decreased PCD. Since PCD is an irreversible decision informed by extensive and unsuccessfully repaired DNA damage, the functional interaction of RBR and NAC044 belongs to a later phase of the DDR than the cell cycle arrest and DNA repair processes, possibly aiding in avoiding the spread of harmful mutations. Two alternative scenarios may explain the decreased PCD when the RBR-NAC044 interaction is disrupted: (1) RBR enhances NAC044 to promote PCD, or (2) NAC044 inhibits RBR protective activity. The exacerbated PCD in the amiGO line is contradictory to the first option but not with the second one, where the residual RBR in the amiGO line is repressed by the relative excess of NAC044. Our data cannot conclusively discriminate between both possibilities due to the independent roles of RBR and NAC044 and the complexity of the DDR networks, leaving an open question for future research.

PCD is a response to genotoxic stress common in plants and animals (Surova & Zhivotovsky, 2013; Szurman-Zubrzycka et al., 2023) that can be executed by several pathways, using different regulators and ultimately leading to different modes of cell death (Prokhorova et al., 2020; Reape et al., 2008; Surova & Zhivotovsky, 2013). Thus, cell fate decisions are intricately linked to the DNA integrity status and if cell survival depends on more than one pathway, cross-talk between them is crucial. The opposite effect of the amiGO and *nac044* single mutants, the intermediate phenotype in the amiGO/*nac044-3* line, the partial decrease in PCD observed in the *NAC044^{GCG}-GFP* lines, and the partial mitigation of the RBR^{NF}-YFP effect by the introgression of *nac044-3* indicate that besides their joint action in promoting PCD, *NAC044*, and *RBR* play independent roles with opposing activities in the regulation of PCD, likely balancing each other to translate the success of repair into a cell fate decision. Accordingly, a complex transcriptional network involving the partially overlapping pathways controlled by SOG1 and E2FA/B deals with DNA replication stress by regulating common targets like BRCA1, RAD51, and NAC044/NAC085 (Nisa et al., 2023). Notably, the E2F transcription factors together with RBR are required for the protective quiescence that prevents stem cells from undergoing PCD upon DNA damage (Cruz-Ramírez et al., 2013; Gombos et al., 2023).

A puzzling observation is the opposite effect of *RBR^{NF}-YFP* on cell death as compared to *NAC044^{GCG}-GFP*. *RBR^{NF}-YFP* rescued the amiGO-induced PCD in unchallenging conditions, but exhibited dominant negative features upon genotoxic stress such as increased cell death and root growth arrest, pointing to an activity switch triggered by induced DNA damage. Additionally, RBR^{NF}-YFP binds E2Fs, of which E2FA is essential for RBR functions in the DDR. Our group has previously shown that (a) E2FA and RBR function in a cell death-inducing DDR independently of SOG1, (b) E2FA is not sufficient on its own, but is necessary to trigger PCD induced by RBR down-regulation and DNA damage, and (c) RBR-E2FA directly repress DDR genes like *BRCA1* under standard growth conditions, but upon genotoxic stress interact even stronger and are required for *BRCA1* activation (Horvath et al., 2017). Taken together with the abovementioned RBR^{NF}-YFP features, it seems that another LXCXE-containing protein is essential for RBR-E2FA to confer protection against genotoxic stress and that RBR-E2FA complexes switch their activity when DNA damage is perceived. Similarly, mammalian p53 promotes a switch from a transcription-activating complex containing the Multi-vulval class B core complex (MuvB), to a repressor DREAM complex which also contains the MuvB proteins, E2F-DP proteins, and the pocket proteins p10/p130 (Engeland, 2018). In the absence of other pocket proteins (Desvoyes, De Mendoza, et al., 2014), Arabidopsis RBR covers the functions of p107/p130 in different DREAM

complexes, which unlike the animal counterpart, can be activating or repressing, the latter of which contains the repressor MYB3R3 proteins (Kobayashi et al., 2015; Ning et al., 2020).

NAC044 controls cell division by promoting the accumulation of repressor MYB3R proteins in response to DNA damage (Takahashi et al., 2019), which in turn bind to the MSA element of G2/M-specific gene promoters to arrest cell cycle progression (Bourbousse et al., 2018; Chen et al., 2017; Ito et al., 1998, 2001; Kobayashi et al., 2015). The mechanism by which NAC044 promotes cell death is less clear, but also involves the repressor MYB3R proteins (Chen et al., 2017; Takahashi et al., 2019) and the binding to RBR, according to our own results. Moreover, NAC044 also interacts with the DREAM complex member LIN37 upon DNA damage (Lang et al., 2021). In turn, the *NAC044* gene displays a DNA damage-induced and cell cycle-dependent expression pattern. Accordingly, MSA, E2FA, and SOG1 binding elements reside in its promoter, and *NAC044*, along with other DDR genes such as *RAD51*, *BRCA1*, *TSO2*, *WEE1*, and *SMR4*, is regulated by SOG1, MYB3R3, E2FA, and RBR (Bourbousse et al., 2018; Bouyer et al., 2018; Kobayashi et al., 2015; Nisa et al., 2023; Ogita et al., 2018; Verkest et al., 2014). Therefore, the SOG1 and RBR DDR pathways converge in a complex set of protein interactions that regulate common DDR targets, among which *NAC044* is a key component of the cross-talk between the two pathways regulating PCD. It will be interesting to investigate whether the age-dependent expression of *NAC044* in the flower abscission zone, which might relate to developmental senescence, is related to its role in PCD.

Altogether, our data indicate that RBR interaction with LXCXE motif-containing proteins is essential for its various functions during the DDR, and might contribute to coordinating them and linking them to the cell fate decision later on. The protein interaction with NAC044 and the regulation of the *NAC044* gene by SOG1 and RBR constitute a cross-talking mechanism between the main DDR pathways in plants. Future research is needed to identify the protein that recruits RBR to nuclear foci, and the dynamic composition of the transcriptional regulatory complexes involving NAC044, E2FA/B, RBR, and other members of the DREAM complex. This knowledge will help to disentangle the complexity of an integrated DDR that ultimately decides whether the cell continues to proliferate or PCD must be activated.

EXPERIMENTAL PROCEDURES

Plant material and growth conditions and treatments

Arabidopsis thaliana ecotype Col-0 was used as wild-type control. All plant lines used are listed in Table S1. Briefly, *nac044-1* (SAIL_1286_D02) (Takahashi et al., 2019), *nac044-3* (WiscDsLox293-296invF22), and *rad54* (SALK124992) were obtained from The Nottingham Arabidopsis Stock Centre (NASC). RAD54-YFP (Hirakawa et al., 2017), E2FA-GFP (Magyar et al., 2012), amiGO-RBR (amiGO), pRBR::RBR:YFP (Cruz-Ramírez et al., 2013), pRBR::RBR:mRFP (Cruz-Ramírez et al., 2012), and pRBR::RBR:sCFP3A (Zamora-Zaragoza et al., 2021) lines were previously published; pRBR::RBR^{NF}:YFP was kindly donated by Sara Diaz-Trivino. Unless otherwise noticed, amiGO was used as background for RBR-YFP and RBR^{NF}-YFP transgenic plants, and *nac044-3* or *nac044-1* for NAC044:GFP and NAC044GCG:GFP as indicated. Transcriptional reporters pNAC044-GUS and pNAC044-3xGFP-NLS are in Col-0. Seeds were fume-sterilized in a sealed container with 100 ml bleach and 3 ml of 37% hydrochloric acid for 3–5 h; then suspended in 0.1% agarose, stratified for 2 days at 4°C in darkness, plated on 0.5× germination medium (GM): (0.5 Murashige and Skoog (MS) plus vitamins, 1% sucrose, 0.5 g L^{-1} 2-(N-morpholino) ethanesulfonic acid (MES) at pH 5.8, and 0.8% plant agar), and grown vertically for the time indicated in each figure legend at 22°C with a 16 h light/8 h dark cycle. For DNA damaging treatments, a filter-sterilized 20 mg ml^{-1} stock solution prepared from zeocin powder (Duchefa Biochemie, Haarlem, The Netherlands) was diluted to 3 μg ml^{-1}, 10 μg ml^{-1}, or 20 μg ml^{-1} in 0.5× MS + vits, 1% sucrose, 0.5 g L^{-1} MES at pH 5.8, 0.8% plant agar before pouring into plates. Seedlings were transferred to zeocin-containing plates for 2, 16, or 20 h as indicated in figure legends before imaging or transfering back to fresh 0.5 GM medium.

Plasmid construction and plant transformation

The constructs pNAC044::GUS, pNAC044::3xGFP:NLS, pNAC044::NAC044:GFP, and pNAC044::NAC044GCG:GFP were cloned using the GreenGate system (Lampropoulos et al., 2013). Briefly, a 980 bp fragment upstream of the ATG was amplified with the primers pANAC044 F and pANAC044 R1 (translational fusion) or pANAC044 R2 (transcriptional fusions); for translational fusions, the genomic segment of NAC044 incuding introns from the ATG but without stop codon (gNAC044) was amplified with the primer pair gANAC044 F/gANAC044 R. Mutagenesis of the of the LXCXE into GXCXG motif was introduced by amplifying gNAC044 in two fragments overlapping at the LXCXE coding sequence with primers pairs gANAC044 F/mut gANAC044 R and mut gANAC044 F/gANAC044 R. Promoter and gNAC044 PCR products were cloned together with the plasmids pGGD001, pGGE009 and pGGF001 (for translational fusion); with pGGB002, pGGC025, pGGD006, pGGE009, and pGGF001 (for 3xGFP-NLS transcriptional fusion); and with pGGB002, pGGC051, pGGD002, pGGE009, pGGF001 (for GUS transcriptional fusion) into the vector pGGZ003 by combining equimolar amounts of each part in 15 μl diglig reactions including 10 mM ATP, 1× Green Buffer (Thermo Fisher, Landsmeer, The Netherlands), 1 μl T4 DNA ligase (30 u μl^{-1}), 1 μl BsaI restriction enzyme (Thermo Fisher) according to the GreenGate protocol. Constructs were transformed into Arabidopsis plants by the flower dip method.

Previously reported and newly generated entry and expression clones are listed in Table S2. The pEXP22-NAC044 expression clone, and the product of a two fragments-overlapping PCR with primers pairs AttB cNAC44 F/mut cNAC44 R and mut cNAC44 F/AttB cNAC44 R that introduce attB sites and mutagenize the LXCXE motif to GXCXG on NAC044 CDS, were recombined into pDONR221 vector with Gateway BP clonase II enzyme mix (Invitrogen) to generate the corresponding entry clones for NAC044 and NAC044^{GCG} CDS. The CDS of E2FA, E2FB, and E2FC, amplified with the corresponding primers listed in Table S3 were cloned into pGEMt-easy 221 vector by BP clonase reaction. We generated pDESTNLuc and pDESTCLuc Gateway-compatible destination vectors by conventional cloning of the attR-flanked Gateway cassette

amplified with the primers GWcass_SplitLUC_F and GWcass_CLuc_R or GWcass_NLuc_R (Table S3) and digested with BpiI restriction enzyme (Thermo Fisher) to generate sticky ends compatible with *Bam*HI/*Sal*I digested pCAMBIA-NLUC and pCAMBIA-CLuc vectors (Chen et al., 2008). Entry clones were recombined into pDEST22 or pDEST32 destination vectors for Y2H assays, and/or into pDESTNLuc or pDESTCLuc for Split-Luciferase assays with Gateway LR clonase II enzyme mix (Invitrogen). For stable transformants of LUCIFERASE and Split-Luc reporters, we used the Golden Gate MoClo system (Engler et al., 2014) and primers listed in Table S3. Briefly, we amplified the promoter and genomic sequences of NAC044 and NAC044^{GCG} from the pGGZ003- pNAC044::NAC044:GFP and pGGZ003-pNAC044::NAC044GCG:GFP constructs (explained above) to clone them into the level 0 vectors pICH41295 (for pNAC044) and pAGM1287 (for either NAC044 or NAC044^{GCG}). The pICH41295-pRBR and pAGM1287-RBR constructs were reported in (Zamora-Zaragoza et al., 2021). Using the pDEST-NLuc and pDEST-CLuc vectors (explained above) as template, we amplified the NLuc and CLuc fragments and cloned them into level 0 vectors pAGM1301 and pAGM1276. Level 0 plasmids were cloned into the level 1 vectors pICH47751 for CLuc-pNAC044::NAC044 constructs and pICH47742 for pRBR::RBR-NLuc. For the LUCIFERASE reporters, we followed the same procedure using the pICSL50006 LUCIFERASE C-terminal tag module from the MoClo system. Level 1 constructs were assembled into level 2 vector pICSL4723 together with the pICSL70008-FAST-R selection cassette; for the Split-Luc system, both RBR-NLuc and CLuc- NAC044 or CLuc NAC044^{GCG} were assembled into a single level 2 construct and transformed into Arabidopsis plants by the flower dip method.

Microscopy and image processing

A 10 μg ml^{-1} Propidium Iodide (PI) staining solution (or mQ water for nuclear foci imaging) was used for whole-mount visualization of live roots with CLSM using a Zeiss LSM 710 system as described in (Zhou et al., 2019); PI, GFP, and YFP were visualized using wavelengths of 600–640 nm, 500–540, and 525–565 nm, respectively. Tissue clearing with ClearSee reagent was performed as described in (Kurihara et al., 2015). In brief, tissues were fixed with 4% w/v paraformaldehyde in 1× PBS for 30 min under vacuum (~690 mmHg) at room temperature, washed twice, and submerged in the Clearsee solution (10% w/v Xylitol powder, 15% (w/v) sodium deoxycholate, and 25% w/v urea dissolved in water) for 1–2 week at room temperature. Images were taken with ZEN 2012 software (Zeiss, Breda, The Netherlands) and processed with ImageJ (V 2.14.0/1.52v). For foci co-localization, images were aligned using the TurboReg registration plugin (Thévenaz et al., 1998), and analyzed using the RGB profiler plugin. Brightness and contrast of the final figures were enhanced to the same values for all comparable panels within the figure. Raw imaging data is available upon request.

Protein–protein interaction assays

Protein–protein interactions by Y2H were performed using the ProQuest system (Thermo Scientific, Bleiswijk, The Netherlands). Co-transformation of pEXP22 and pEXP32 expression clones (Table S2) into the PJ69-4A yeast strain was performed as described in (De Folter & Immink, 2011). Transient Split-Luciferase assays in *Nicothiana benthamiana* leaves (Table S2) were performed as described in Chen et al. (2008) using an exposure time of 7 min; inserts are expressed under CaMV35S promoter. For Split-Luc in Arabidopsis stable transformants (Table S1), we used an exposure time of 10 min; inserts are expressed under their own promoter (pRBR or pNAC044). Luciferase activity was detected after spraying with 1 mM D-luciferin (Duchefa Biochemie) using an (−80°C) air-cooled CCD Pixis 1024B camera system (Princeton Instruments, Massachusetts, USA) equipped with a 35 mm, 1:1.4 Nikkon SLR camera lens (Nikon, Tokyo, Japan) fitted with a DT Green filter ring (Image Optics Components Ltd, Orsay, France) to block chlorophyll fluorescence. Luciferase images were processed using a 'Fire' lookup table in ImageJ Software, adjusting brightness and contrast to the same values in all images.

Protein sequence retrieval and alignments

Arabidopsis thaliana NAC044, NAC085, and RAD54 protein sequences were retrieved from The Arabidopsis Information Resource (TAIR, arabidopsis.org) and used as query to BLAST search on Gramene.org for plant orthologs, or on NCBI for non-plant orthologs. Annotated orthologs or the top score hit sequences were retrieved and aligned with Clustal-omega (https://www.ebi.ac.uk/Tools/msa/clustalo/) to the Arabidopsis sequences.

Quantification and statistical analysis

Statistical parameters and tests are mentioned in figure legends. Calculations were done using GraphPad Prism software 5.0 (GraphPad Software, San Diego, CA, USA) and R-based statistical analyses.

ACKNOWLEDGEMENTS

We thank Prof. Lieven De Veylder (VIB-UGent Center for Plant Systems Biology) for his valuable suggestions on this manuscript, and for sharing plasmid material; to Prof. Sachihiro Matsunaga (Tokyo University of Science) for sharing the RAD54-EYFP line; Dr. Yessica Alina Rodríguez-Rosales (Radboud UMC) for her support with statistical analysis and R plots. WZ was supported by the National Natural Science Foundation of China (32070874); JZZ was supported by Consejo Nacional de Ciencia y Tecnología (CONACyT, Mexico, 383871).

CONFLICT OF INTEREST

The authors declare that they have no conflict of interest.

DATA AVAILABILITY STATEMENT

All relevant data can be found within the manuscript and its supporting materials.

SUPPORTING INFORMATION

Additional Supporting Information may be found in the online version of this article.

Figure S1. RBRNF-YFP is sensitive to zeocin treatment and fails to form zeocin-induced foci.

Figure S2. RAD54 and RBR act independently in DNA damage repair.

Figure S3. *In planta* Split-LUCIFERASE assays show that RBRNF interacts with E2F proteins and NAC044 interacts with RBR through the LXCXE motif.

Figure S4. NAC044 is expressed after DNA damage, does not recruit RBR to nuclear foci, and inhibits root growth.

Figure S5. RBRNF dominantly affects the DNA damage response through a different mechanism than binding NAC044.

Table S1. Plant lines.

Table S2. Plasmids and vectors.

Table S3. Primers.

REFERENCES

Berckmans, B. & **De Veylder, L.** (2009) Transcriptional control of the cell cycle. *Current Opinion in Plant Biology*, **12**, 599–605.

Biedermann, S., **Harashima, H.**, **Chen, P.**, **Heese, M.**, **Bouyer, D.**, **Sofroni, K.** ***et al.*** (2017) The retinoblastoma homolog RBR1 mediates localization of the repair protein RAD51 to DNA lesions in Arabidopsis. *The EMBO Journal*, **36**, 1279–1297.

Boniotti, M.B. & **Gutierrez, C.** (2001) A cell-cycle-regulated kinase activity phosphorylates plant retinoblastoma protein and contains, in Arabidopsis, a CDKA/cyclin D complex. *The Plant Journal*, **28**, 341–350.

Bourbousse, C., **Vegesna, N.** & **Law, J.A.** (2018) SOG1 activator and MYB3R repressors regulate a complex DNA damage network in Arabidopsis. *Proceedings of the National Academy of Sciences of the United States of America*, **115**, E12453–E12462.

Bourgo, R.J., **Thangavel, C.**, **Ertel, A.**, **Bergseid, J.**, **Kathleen McClendon, A.**, **Wilkens, L.** ***et al.*** (2011) RB restricts DNA damage-initiated tumorigenesis through an LXCXE-dependent mechanism of transcriptional control. *Molecular Cell*, **43**, 663–672.

Bouyer, D., **Heese, M.**, **Chen, P.**, **Harashima, H.**, **Roudier, F.**, **Gruttner, C.** ***et al.*** (2018) Genome-wide identification of RETINOBLASTOMA RELATED 1 binding sites in Arabidopsis reveals novel DNA damage regulators. *PLoS Genetics*, **14**, 1–35.

Chen, H., **Zou, Y.**, **Shang, Y.**, **Lin, H.**, **Wang, Y.**, **Cai, R.** ***et al.*** (2008) Firefly luciferase complementation imaging assay for protein-protein interactions in plants. *Plant Physiology*, **146**, 368–376.

Chen, J. (2016) The cell-cycle arrest and apoptotic functions of p53 in tumor initiation and progression. *Cold Spring Harbor Perspectives in Medicine*, **6**, 1–16.

Chen, P., **Sjogren, C.A.**, **Larsen, P.B.** & **Schnittger, A.** (2019) A multi-level response to DNA damage induced by aluminium. *The Plant Journal*, **98**, 479–491.

Chen, P., **Takatsuka, H.**, **Takahashi, N.**, **Kurata, R.**, **Fukao, Y.**, **Kobayashi, K.** ***et al.*** (2017) Arabidopsis R1R2R3-Myb proteins are essential for inhibiting cell division in response to DNA damage. *Nature Communications*, **8**, 1–12.

Chen, T. & **Wang, J.Y.J.** (2000) Establishment of irreversible growth arrest in myogenic differentiation requires the RB LXCXE-binding function. *Molecular and Cellular Biology*, **20**, 5571–5580.

Chen, Z., **Higgins, J.D.**, **Hui, J.T.L.**, **Li, J.**, **Franklin, F.C.H.** & **Berger, F.** (2011) Retinoblastoma protein is essential for early meiotic events in *Arabidopsis*. *The EMBO Journal*, **30**, 744–755.

Ciccia, A. & **Elledge, S.J.** (2010) The DNA damage response: making it safe to play with knives. *Molecular Cell*, **40**, 179–204.

Clay, D.E. & **Fox, D.T.** (2021) DNA damage responses during the cell cycle: insights from model organisms and beyond. *Genes (Basel)*, **12**, 1882.

Cruz-Ramírez, A., **Díaz-Triviño, S.**, **Blilou, I.**, **Grieneisen, V.A.**, **Sozzani, R.**, **Zamioudis, C.** ***et al.*** (2012) A Bistable circuit involving SCARECROW-RETINOBLASTOMA integrates cues to inform asymmetric stem cell division. *Cell*, **150**, 1002–1015.

Cruz-Ramírez, A., **Diaz-trivino, S.**, **Wachsman, G.**, **Du, Y.**, **Arteaga-Vazquez, M.**, **Zhang, H.** ***et al.*** (2013) A SCARECROW-RETINOBLASTOMA protein network controls protective quiescence in the Arabidopsis root stem cell organizer. *PLoS Biology*, **11**, e1001724.

De Folter, S. & **Immink, R.G.H.** (2011) Yeast protein-protein interaction assays and screens. *Methods in Molecular Biology*, **754**, 145–165.

De Veylder, L., **Beeckman, T.**, **Beemster, G.T.S.**, **De Almeida Engler, J.**, **Ormenese, S.**, **Maes, S.** ***et al.*** (2002) Control of proliferation, endoreduplication and differentiation by the Arabidopsis E2Fa-DPa transcription factor. *The EMBO Journal*, **21**, 1360–1368.

DeCaprio, J.A. (2009) How the Rb tumor suppressor structure and function was revealed by the study of Adenovirus and SV40. *Virology*, **384**, 274–284.

Desvoyes, B., **De Mendoza, A.**, **Ruiz-Trillo, I.** & **Gutierrez, C.** (2014) Novel roles of plant RETINOBLASTOMA-RELATED (RBR) protein in cell proliferation and asymmetric cell division. *Journal of Experimental Botany*, **65**, 2657–2666.

Desvoyes, B., **Fernández-marcos, M.**, **Sequeira-mendes, J.**, **Otero, S.**, **Vergara, Z.** & **Gutierrez, C.** (2014) Looking at plant cell cycle from the chromatin window. *Frontiers in Plant Science*, **5**, 369.

Desvoyes, B. & **Gutierrez, C.** (2020) Roles of plant retinoblastoma protein: cell cycle and beyond. *The EMBO Journal*, **39**, 1–18.

Dick, F.A. & **Rubin, S.M.** (2013) Molecular mechanisms underlying RB protein function. *Nature Reviews. Molecular Cell Biology*, **14**, 297–306.

Ebel, C., **Mariconti, L.** & **Gruissem, W.W.** (2004) Plant retinoblastoma homologues control nuclear proliferation in the female gametophyte. *Nature*, **429**, 776–780.

Engeland, K. (2018) Cell cycle arrest through indirect transcriptional repression by p53: I have a DREAM. *Cell Death and Differentiation*, **25**, 114–132.

Engler, C., **Youles, M.**, **Gruetzner, R.**, **Ehnert, T.M.**, **Werner, S.**, **Jones, J.D.G.** ***et al.*** (2014) A Golden Gate modular cloning toolbox for plants. *ACS Synthetic Biology*, **3**, 839–843.

Flemington, E.K., **Speck, S.H.** & **Kaelin, W.G.** (1993) E2F-1-mediated transactivation is inhibited by complex formation with the retinoblastoma susceptibility gene product. *Proceedings of the National Academy of Sciences of the United States of America*, **90**, 6914–6918.

Gentric, N., **Masoud, K.**, **Journot, R.P.**, **Cognat, V.**, **Chabouté, M.E.**, **Noir, S.** ***et al.*** (2020) The f-box-like protein FBL17 is a regulator of DNA-damage response and colocalizes with RETINOBLASTOMA RELATED1 at DNA lesion sites. *Plant Physiology*, **183**, 1295–1305.

Gombos, M., **Raynaud, C.**, **Nomoto, Y.**, **Molnár, E.**, **Brik-Chaouche, R.**, **Takatsuka, H.** ***et al.*** (2023) The canonical E2Fs together with RETINOBLASTOMA-RELATED are required to establish quiescence during plant development. *Communications Biology*, **6**, 1–15.

Gutzat, R., **Borghi, L.** & **Gruissem, W.** (2012) Emerging roles of RETINOBLASTOMA-RELATED proteins in evolution and plant development. *Trends in Plant Science*, **17**, 139–148.

Harashima, H. & **Sugimoto, K.** (2016) Integration of developmental and environmental signals into cell proliferation and differentiation through RETINOBLASTOMA-RELATED 1. *Current Opinion in Plant Biology*, **29**, 95–103.

Helin, K., **Harlow, E.D.** & **Fattaey, A.L.** (1993) Inhibition of E2F-1 transactivation by direct binding of the retinoblastoma protein. *Molecular and Cellular Biology*, **13**, 6501–6508.

Hirakawa, T., **Hasegawa, J.**, **White, C.I.** & **Matsunaga, S.** (2017) RAD54 forms DNA repair foci in response to DNA damage in living plant cells. *The Plant Journal*, **90**, 372–382.

Hirakawa, T. & **Matsunaga, S.** (2019) Characterization of DNA repair foci in root cells of Arabidopsis in response to DNA damage. *Frontiers in Plant Science*, **10**, 990.

Horvath, B.M., **Kourova, H.**, **Nagy, S.**, **Nemeth, E.**, **Magyar, Z.**, **Papdi, C.** ***et al.*** (2017) Arabidopsis RETINOBLASTOMA RELATED directly regulates DNA damage responses through functions beyond cell cycle control. *The EMBO Journal*, **36**, 1261–1278.

Hu, Z., **Cools, T.** & **De Veylder, L.** (2016) Mechanisms used by plants to cope with DNA damage. *Annual Review of Plant Biology*, **67**, 439–462.

Ito, M., **Araki, S.**, **Matsunaga, S.**, **Itoh, T.**, **Nishihama, R.**, **Machida, Y.** ***et al.*** (2001) G2/M-phase-specific transcription during the plant cell cycle is mediated by c-Myb-like transcription factors. *Plant Cell*, **13**, 1891–1905.

Ito, M., **Iwase, M.**, **Kodama, H.**, **Lavisse, P.**, **Komamine, A.**, **Nishihama, R.** ***et al.*** (1998) A novel cis-acting element in promoters of plant B-type cyclin genes activates M phase-specific transcription. *Plant Cell*, **10**, 331–341.

Johnston, A.J., **Matveeva, E.**, **Kirioukhova, O.**, **Grossniklaus, U.** & **Gruissem, W.** (2008) A dynamic reciprocal RBR-PRC2 regulatory circuit controls Arabidopsis gametophyte development. *Current Biology*, **18**, 1680–1686.

Kastenhuber, E.R. & **Lowe, S.W.** (2017) Putting p53 in context. *Cell*, **170**, 1062–1078.

Kim, J.H., **Ryu, T.H.**, **Lee, S.S.**, **Lee, S.** & **Chung, B.Y.** (2019) Ionizing radiation manifesting DNA damage response in plants: an overview of DNA damage signaling and repair mechanisms in plants. *Plant Science*, **278**, 44–53.

Kobayashi, K., **Suzuki, T.**, **Iwata, E.**, **Nakamichi, N.**, **Suzuki, T.**, **Chen, P.** ***et al.*** (2015) Transcriptional repression by MYB 3R proteins regulates plant organ growth. *The EMBO Journal*, **34**, 1992–2007.

Kurihara, D., **Mizuta, Y.**, **Sato, Y.** & **Higashiyama, T.** (2015) ClearSee: a rapid optical clearing reagent for whole-plant fluorescence imaging. *Development*, **142**, 4168–4179.

Lampropoulos, A., **Sutikovic, Z.**, **Wenzl, C.**, **Maegele, I.**, **Lohmann, J.U.** & **Forner, J.** (2013) GreenGate - a novel, versatile, and efficient cloning system for plant transgenesis. *PLoS One*, **8**, e83043.

Lang, L., **Pettkó-Szandtner, A.**, **Elbasi, H.T.**, **Takatsuka, H.**, **Nomoto, Y.**, **Zaki, A.** ***et al.*** (2021) The DREAM complex represses growth in response to DNA damage in Arabidopsis. *Life Science Alliance*, **4**, 1–20.

Lanz, M.C., **Dibitetto, D.** & **Smolka, M.B.** (2019) DNA damage kinase signaling: checkpoint and repair at 30 years. *The EMBO Journal*, **38**, e101801.

Magyar, Z., **Horváth, B.**, **Khan, S.**, **Mohammed, B.**, **Henriques, R.**, **De Veylder, L.** ***et al.*** (2012) Arabidopsis E2FA stimulates proliferation and endocycle separately through RBR-bound and RBR-free complexes. *The EMBO Journal*, **31**, 1480–1493.

Mahapatra, K. & **Roy, S.** (2020) An insight into the mechanism of DNA damage response in plants- role of SUPPRESSOR OF GAMMA RESPONSE 1: an overview. *Mutation Research - Fundamental and Molecular Mechanisms of Mutagenesis*, **819–820**, 111689.

Nakagami, H., **Kawamura, K.**, **Sugisaka, K.**, **Sekine, M.** & **Shinmyo, A.** (2002) Phosphorylation of retinoblastoma-related protein by the cyclin D/cyclin-dependent kinase complex is activated at the G1/S-phase transition in tobacco. *Plant Cell*, **14**, 1847–1857.

Nakamura, A.J., **Rao, V.A.**, **Pommier, Y.** & **Bonner, W.M.** (2010) The complexity of phosphorylated H2AX foci formation and DNA repair assembly at DNA double-strand breaks. *Cell Cycle*, **9**, 389–397.

Narasimha, A.M., **Kaulich, M.**, **Shapiro, G.S.**, **Choi, Y.J.**, **Sicinski, P.** & **Dowdy, S.F.** (2014) Cyclin D activates the Rb tumor suppressor by mono-phosphorylation. *eLife*, **3**, 1–21.

Ning, Y., **Liu, N.**, **Lan, K.**, **Su, Y.**, **Li, L.**, **Chen, S.** ***et al.*** (2020) DREAM complex suppresses DNA methylation maintenance genes and precludes DNA hypermethylation. *Nature Plants*, **6**, 942–956.

Nisa, M., **Eekhout, T.**, **Bergis, C.**, **Pedroza-Garcia, J.A.**, **He, X.**, **Mazubert, C.** ***et al.*** (2023) Distinctive and complementary roles of E2F transcription factors during plant replication stress responses. *Molecular Plant*, **16**, 1269–1282.

Nisa, M.U., **Huang, Y.**, **Benhamed, M.** & **Raynaud, C.** (2019) The plant DNA damage response: signaling pathways leading to growth inhibition and putative role in response to stress conditions. *Frontiers in Plant Science*, **10**, 1–12.

Ogita, N., **Okushima, Y.**, **Tokizawa, M.**, **Yamamoto, Y.Y.**, **Tanaka, M.**, **Seki, M.** ***et al.*** (2018) Identifying the target genes of SUPPRESSOR OF GAMMA RESPONSE 1, a master transcription factor controlling DNA damage response in Arabidopsis. *The Plant Journal*, **94**, 439–453.

Perilli, S., **Perez-Perez, J.M.**, **Di Mambro, R.**, **Peris, C.L.**, **Díaz-Triviño, S.**, **Del Bianco, M.** ***et al.*** (2013) RETINOBLASTOMA-RELATED protein stimulates cell differentiation in the Arabidopsis root meristem by interacting with cytokinin signaling. *Plant Cell*, **25**, 4469–4478.

Polit, J.T., **Kaźmierczak, A.** & **Walczak-Drzewiecka, A.** (2012) Cell cycle-dependent phosphorylation of pRb-like protein in root meristem cells of Vicia faba. *Protoplasma*, **249**, 131–137.

Polo, S.E. & **Jackson, S.P.** (2011) Dynamics of DNA damage response proteins at DNA breaks: a focus on protein modifications. *Genes & Development*, **25**, 409–433.

Prokhorova, E.A., **Egorshina, A.Y.**, **Zhivotovsky, B.** & **Kopeina, G.S.** (2020) The DNA-damage response and nuclear events as regulators of nonapoptotic forms of cell death. *Oncogene*, **39**, 1–16.

Pruneda-Paz, J.L.L., **Breton, G.**, **Nagel, D.H.H.**, **Kang, S.E.E.**, **Bonaldi, K.**, **Doherty, C.J.J.** ***et al.*** (2014) A genome-scale resource for the functional characterization of Arabidopsis transcription factors. *Cell Reports*, **8**, 622–632.

Reape, T.J., **Molony, E.M.** & **McCabe, P.F.** (2008) Programmed cell death in plants: distinguishing between different modes. *Journal of Experimental Botany*, **59**, 435–444.

Rubin, S.M. (2013) Deciphering the retinoblastoma protein phosphorylation code. *Trends in Biochemical Sciences*, **38**, 12–19.

Sanidas, I., **Morris, R.**, **Fella, K.A.**, **Rumde, P.H.**, **Boukhali, M.**, **Tai, E.C.** ***et al.*** (2019) A code of mono-phosphorylation modulates the function of RB. *Molecular Cell*, **73**, 985–1000.e6.

Surova, O. & **Zhivotovsky, B.** (2013) Various modes of cell death induced by DNA damage. *Oncogene*, **32**, 3789–3797.

Szurman-Zubrzycka, M., **Jędrzejek, P.** & **Szarejko, I.** (2023) How do plants cope with DNA damage? A concise review on the DDR pathway in plants. *International Journal of Molecular Sciences*, **24**, 2404.

Takahashi, N., **Ogita, N.**, **Takahashi, T.**, **Taniguchi, S.**, **Tanaka, M.**, **Seki, M.** ***et al.*** (2019) A regulatory module controlling stress-induced cell cycle arrest in Arabidopsis. *eLife*, **8**, 1–27.

Thévenaz, P., **Ruttimann, U.E.** & **Unser, M.** (1998) A pyramid approach to subpixel registration based on intensity. *IEEE Transactions on Image Processing*, **7**, 27–41.

Tsegay, P.S., **Lai, Y.** & **Liu, Y.** (2019) Replication stress and consequential instability of the genome and epigenome. *Molecules*, **24**, 1–20.

Vélez-Cruz, R., **Manickavinayaham, S.**, **Biswas, A.K.**, **Clary, R.W.**, **Premkumar, T.**, **Cole, F.** ***et al.*** (2016) RB localizes to DNA double-strand breaks and promotes DNA end resection and homologous recombination through the recruitment of BRG1. *Genes & Development*, **30**, 2500–2512.

Verkest, A., **Abeel, T.**, **Heyndrickx, K.S.**, **Van Leene, J.**, **Lanz, C.**, **Van De Slijke, E.** ***et al.*** (2014) A generic tool for transcription factor target gene discovery in Arabidopsis cell suspension cultures based on tandemchromatinaffinity purification. *Plant Physiology*, **164**, 1122–1133.

Waterworth, W.M., **Wilson, M.**, **Wang, D.**, **Nuhse, T.**, **Warward, S.**, **Selley, J.** ***et al.*** (2019) Phosphoproteomic analysis reveals plant DNA damage signalling pathways with a functional role for histone H2AX phosphorylation in plant growth under genotoxic stress. *The Plant Journal*, **100**, 1007–1021.

Wildwater, M., **Campilho, A.**, **Perez-Perez, J.M.**, **Heidstra, R.**, **Blilou, I.**, **Korthout, H.** ***et al.*** (2005) The RETINOBLASTOMA-RELATED gene regulates stem cell maintenance in Arabidopsis roots. *Cell*, **123**, 1337–1349.

Williams, A.B. & **Schumacher, B.** (2016) p53 in the DNA-damage-repair process. *Cold Spring Harbor Perspectives in Medicine*, **6**, 1–16.

Yi, D., **Kamei, C.L.A.**, **Cools, T.**, **Vanderauwera, S.**, **Takahashi, N.**, **Okushima, Y.** ***et al.*** (2014) The Arabidopsis SIAMESE-RELATED cyclin-dependent kinase inhibitors SMR5 and SMR7 regulate the DNA damage checkpoint in response to reactive oxygen species. *Plant Cell*, **26**, 296–309.

Yoshiyama, K., **Conklin, P.A.**, **Huefner, N.D.** & **Britt, A.B.** (2009) Suppressor of gamma response 1 (SOG1) encodes a putative transcription factor governing multiple responses to DNA damage. *Proceedings of the National Academy of Sciences of the United States of America*, **106**, 12843–12848.

Zamora-Zaragoza, J., **Klap, K.**, **Sánchez-Pérez, J.**, **Vielle-Calzada, J.P.** & **Scheres, B.** (2021) A phosphorylation code regulates the multi-functional protein RETINOBLASTOMA-RELATED1 in Arabidopsis thaliana. *BioRxiv*.

Zhou, W., **Lozano-Torres, J.L.**, **Blilou, I.**, **Zhang, X.**, **Zhai, Q.**, **Smant, G.** ***et al.*** (2019) A Jasmonate signaling network activates root stem cells and promotes regeneration. *Cell*, **177**, 942–956.e14.